Aqueous Stability of Mesoporous Silica Films Doped or Grafted with Aluminum Oxide

Darren R. Dunphy,[†] Sarany Singer,[†] Adam W. Cook,[†] Bernd Smarsly,[‡]
Dhaval A. Doshi,[‡] and C. Jeffrey Brinker*,[†,‡]

*Sandia National Laboratories, Advanced Materials Laboratory, 1001 University Boulevard
SE, Albuquerque, New Mexico 87106, and University of New Mexico, Center for
Micro-Engineered Materials, Department of Chemical & Nuclear Engineering,
Albuquerque, New Mexico 87106*

Surfactant-templated silica thin films are potentially important materials for applications such as chemical sensing. However, a serious limitation for their use in aqueous environments is their poor hydrolytic stability. One convenient method of increasing the resistance of mesoporous silica to water degradation is addition of alumina, either doped into the pore walls during material synthesis or grafted onto the pore surface of preformed mesophases. Here, we compare these two routes to Al-modified mesoporous silica with respect to their effectiveness in decreasing the solubility of thin mesoporous silicate films. Direct synthesis of templated silica films prepared with Al/Si = 1:50 was found to limit film degradation, as measured by changes in film thickness, to less than 15% at near-neutral pH over a 1 week period. In addition to suppressing film dissolution, addition of Al can also cause structural changes in silica films templated with the nonionic surfactant Brij 56 ($C_{16}H_{33}(OCH_2CH_2)_{n\sim10}OH$), including mesophase transformation, a decrease in accessible porosity, and an increase in structural disorder. The solubility behavior of films is also sensitive to their particular mesophase, with 3D phases (cubic, disordered) possessing less internal but more thickness stability than 2D phases (hexagonal), as determined with ellipsometric measurements. Finally, grafting of Al species onto the surface of surfactant-templated silica films also significantly increases aqueous stability, although to a lesser extent than the direct synthesis route.

Introduction

Thin films of mesoporous silica, fabricated via the evaporation-induced self-assembly (EISA) of sols containing a surfactant template,[1–3] are a promising technology for applications such as chemical sensing,[4–6] low-*k* dielectrics,[7,8] analyte preconcentration,[9] and low refractive index optical claddings.[10,11] Compared to nontemplated sol–gel materials, surfactant-templated films possess comparable porosites, a narrower pore-size distribution, and pore dimensions and connectivities that are easily controlled by choice of surfactant template. In addition, although surfactant-templated structures are generally less porous than aerogel materials, the small pore size and narrow pore-size distribution of the former greatly decrease optical scattering and film roughness. Finally, EISA is rapid and is amenable to spatial definition by techniques such as inkjet printing,[12] micromolding,[12] or even optical patterning.[13]

A potential limitation of mesoporous silica films is their low stability in aqueous media, however. A 1 cm² film with a thickness of 1 μm and a porosity of 50% contains just 0.11 mg of SiO_2; given a solubility of ~100 ppm for amorphous silica at room temperature and neutral pH, this amount of silica will dissolve in just a little over 1 mL of water. This same phenomenon has been observed in mesoporous silica powders (i.e. MCM-41 or MCM-48),[14–21] where hydrothermal stability is critical for applications in catalysis. A number of strategies have been implemented in order to produce powdered materials that are more robust in the presence of water (at both low and high temperatures), including increasing pore wall thickness,[17] addition of salts during material synthesis,[14,19] and postsynthesis derivitization with organically modified

* Corresponding author. E-mail: cjbrink@sandia.gov.
† Sandia National Laboratories.
‡ University of New Mexico.
(1) Lu, Y. F.; Ganguli, R.; Drewien, C. A.; Anderson, M. T.; Brinker, C. J.; Gong, W. L.; Guo, Y. X.; Soyez, H.; Dunn, B.; Huang, M. H.; Zink, J. I. *Nature* **1997,** *389,* 364–368.
(2) Lu, Y. F.; Fan, H. Y.; Doke, N.; Loy, D. A.; Assink, R. A.; LaVan, D. A.; Brinker, C. J. *J. Am. Chem. Soc.* **2000,** *122,* 5258–5261.
(3) Sellinger, A.; Weiss, P. M.; Nguyen, A.; Lu, Y. F.; Assink, R. A.; Gong, W. L.; Brinker, C. J. *Nature* **1998,** *394,* 256–260.
(4) Innocenzi, P.; Martucci, A.; Guglielmi, M.; Bearzotti, A.; Traversa, E. *Sens. Actuators, B: Chem.* **2001,** *76,* 299–303.
(5) Yamada, T.; Zhou, H.-S.; Uchida, H.; Tomita, M.; Ueno, Y.; Ichino, T.; Honma, I.; Asai, K.; Katsube, T. *Adv. Mater.* **2002,** *14,* 812–815.
(6) Wirnsberger, G.; Scott, B. J.; Stucky, G. D. *Chem. Commun.* **2001,** 119–120.
(7) Baskaran, S.; Liu, J.; Domansky, K.; Kohler, N.; Li, X.; Coyle, C.; Fryxell, G. E.; Thevuthasan, S.; Williford, R. E. *Adv. Mater.* **2000,** *12,* 291–294.
(8) Fan, H. Y.; Bentley, H. R.; Kathan, K. R.; Clem, P.; Lu, Y. F.; Brinker, C. J. *J. Non-Cryst. Solids* **2001,** *285,* 79–83.
(9) Lu, Y. F.; Han, L.; Brinker, C. J.; Niemczyk, T. M.; Lopez, G. P. *Sens. Actuators, B: Chem.* **1996,** *36,* 517–521.
(10) Wirnsberger, G.; Yang, P. D.; Scott, B. J.; Chmelka, B. F.; Stucky, G. D. *Spectrochim. Acta A* **2001,** *57,* 2049–2060.
(11) Yang, P. D.; Wirnsberger, G.; Huang, H. C.; Cordero, S. R.; McGehee, M. D.; Scott, B.; Deng, T.; Whitesides, G. M.; Chmelka, B. F.; Buratto, S. K.; Stucky, G. D. *Science* **2000,** *287,* 465–467.

(12) Fan, H. Y.; Lu, Y. F.; Stump, A.; Reed, S. T.; Baer, T.; Schunk, R.; Perez-Luna, V.; Lopez, G. P.; Brinker, C. J. *Nature* **2000,** *405,* 56–60.
(13) Doshi, D. A.; Huesing, N. K.; Lu, M. C.; Fan, H. Y.; Lu, Y. F.; Simmons-Potter, K.; Potter, B. G.; Hurd, A. J.; Brinker, C. J. *Science* **2000,** *290,* 107–111.
(14) Das, D.; Tsai, C.-M.; Cheng, S. *Chem. Commun.* **1999,** 473–474.
(15) Mokaya, R. *J. Phys. Chem. B* **2000,** *104,* 8279–8286.
(16) Chen, L. Y.; Jaenicke, S.; Chuah, G. K. *Microporous Mesoporous Mater.* **1997,** *12,* 323–330.
(17) Mokaya, R. *Chem. Commun.* **2001,** 633–634.
(18) Kawi, S.; Shen, S. C. *Mater. Lett.* **2000,** *42,* 108–112.
(19) Kim, J. M.; Jun, S.; Ryoo, R. *J. Phys. Chem. B* **1999,** *103,* 6200–6205.
(20) Ribeiro Carrott, M. M. L.; Estêvaõ Candeias, A. J.; Carrott, P. J. M.; Unger, K. K. *Langmuir* **1999,** *15,* 8895–8901.
(21) Zhao, X. S.; Audsley, F.; Lu, G. Q. *J. Phys. Chem. B* **1998,** *102,* 4143–4146.

silanes.[22] Arguably the most attractive route to improving hydrolytic stability, however, is addition of secondary metal oxides to purely siliceous materials, either during material formation or during a postsynthesis grafting step.[15,16,18,23,34] Metals that have been investigated for this purpose include Fe, La,[26] Ti,[16] and Al, with the latter being the most common. For Al, both grafting[23,24,28,30−32] and direct synthesis[15,18,23−25,31−35] routes have been found to be highly effective in increasing hydrolytic stability for powdered mesoporous silica materials. For this reason, we have chosen this strategy to increase the aqueous stability of mesoporous silica thin films.

In this report, we demonstrate that, using a direct synthesis route where an alumina precursor is added to a silica sol before film deposition, inclusion of even 0.5% Al (by mole ratio) into a surfactant-templated silica mesophase greatly increases film stability in water, with a maximum stability reached at ~2% Al/Si. As well as imparting aqueous stability, addition of Al is also shown to induce structural changes in films templated with Brij 56. Although the exact mechanism whereby stability is endowed in mesoporous silica films by Al doping is unknown, it is clear that mesophase identity plays a major role; a comparison of dissolution rates between films templated with different surfactants or with the same surfactant at different concentrations (all at constant Al/Si ratios) clearly indicates that mesophase identity influences the rate of dissolution. Finally, the direct synthesis route to Al-doped SiO_2 films is compared with the solution-phase grafting of Al species onto preformed mesoporous silica thin films. The grafting method was found to be slightly inferior to the direct synthesis route in terms of creating resistance to film dissolution, while also increasing processing complexity. Grafting does appear to be less likely to perturb mesostructure, however.

Although the focus of this paper is the effect of film composition and structure on aqueous stability, it should be noted that film solubility is a function of many more parameters than are discussed here, including temperature,[36] solution composition and pH,[36,37] concentration of dissolved silica,[36] and so forth. In general, results obtained on our films under different conditions parallel those obtained on other silica materials (decreased solubility at lower pH, suppression of dissolution by addition of dissolved $Si(OH)_4$, increased solubility with increasing ionic strength, etc.).

Experimental Section

Materials. All chemicals were used as received. Tetraethyl orthosilicate (TEOS), Brij 56, and cetyltrimethylammonium bromide (CTAB) were obtained from Aldrich, while $AlCl_3$ and $AlCl_3\cdot6H_2O$ were manufactured by J.T. Baker. The triblock template Pluronic P123 was donated by BASF Corp. Tris-(hydroxymethyl)aminoethane (Tris) was acquired from Sigma. Finally, hydrochloric acid was VWR brand, while absolute ethanol was obtained from Aaper. Millipore deionized water was used for all experiments.

Film Synthesis. Films were synthesized using a two-step process. First, a silica precursor stock solution was prepared by heating tetraethyl orthosilicate, absolute ethanol, H_2O, and HCl (in mole ratios of $1:4:1:5 \times 10^{-5}$, respectively) to 60 °C for 90 min. For Al-doped films produced by the direct synthesis route, this stock solution was added to a solution of ethanol, HCl, and surfactant, and then the resulting solution was slowly poured into a vial containing an appropriate amount of $AlCl_3$. *Caution: Care must be taken in this procedure, as the reaction between $AlCl_3$ and water or ethanol is highly exothermic and produces copious HCl vapor.* This addition sequence was chosen solely for purposes of convenience and not for any known effects on final film structure. The final molar composition of this solution was 1 Si:8 ethanol:5 H_2O:0.75 HCl:0−0.04 Al, with either 0.021 or 0.042 g of surfactant (Brij 56, P123, CTAB) added per milliliter of solution. The molar ratio for HCl does not include acid generated from the reaction of $AlCl_3$; it appeared that much of this was lost as vapor. Nonetheless, inclusion of this HCl at the maximum Al concentration we investigated only raises the above HCl ratio to 0.85, a pH change of less than 0.1 pH units. Films were formed by spin coating onto silicon substrates at 2000 rpm for 30 s, at a relative humidity of 25−30%. The surfactant template was removed by calcination at 450 °C for 3 h (1 °C/min heating ramp rate).

A sol of identical composition as above (minus the $AlCl_3$) was used to deposit films for surface grafting. These films were templated with 0.042 g of Brij 56/mL of sol. After calcination, Al was grafted by immersing films in ~25 mL of 0.5 M $AlCl_3\cdot6H_2O$ per sample at 80 °C for 1−11 h. After being removed from this solution, films were rinsed with DI H_2O and thermally treated a second time under the same conditions as those for the primary calcination to chemically bond grafted Al species to the silica surface.

Characterization. Refractive index and thickness measurements were made with a J.A. Wollam Co. M44 spectroscopic ellipsometer using a Cauchy dispersion model to determine film optical constants. Refractive index profiles were assumed to be step-index, corresponding to a homogeneous film structure. All refractive index values (reported at a wavelength of 632.5 nm) and thickness measurements were made in triplicate and averaged to obtain the data points reported herein.

X-ray diffraction (XRD) was performed on a Siemens D-500 diffractometer, using a Cu Kα source. Small-angle X-ray scattering (SAXS) measurements were made using a grazing incidence geometry with a SAXS pinhole instrument at the University of New Mexico/Sandia National Laboratories small-angle scattering laboratory. Experimental details of this instrument are given elsewhere.[38]

Nitrogen adsorption isotherms were collected using an in-house designed 96 MHz surface acoustic wave (SAW) apparatus[39−41] interfaced with a Micromeritics ASAP 2010 surface area and porosimetry analyzer. Films were deposited on SAW substrates under conditions identical to those used for films made for ellipsometric and X-ray analysis.

TEM was used to directly image the mesostructure. TEM was performed on a JEOL 2010, operating at an accelerating voltage of 200 kV and equipped with a Gatan slow scan CCD camera.

(22) Koyano, K. A.; Tatsumi, T.; Tanaka, Y.; Nakata, S. *J. Phys. Chem. B* **1997**, *101*, 9436−9440.

(23) Chen, L. Y.; Ping, Z.; Chuah, G. K.; Jaenicke, S.; Simon, G. *Microporous Mesoporous Mater.* **1999**, *27*, 231−242.

(24) Ghanbari-Siahkali, A.; Philippou, A.; Garforth, A.; Cundy, C. S.; Anderson, M. W.; Dwyer, J. *J. Mater. Chem.* **2000**, *11*, 569−577.

(25) Han, Y.; Wu, S.; Sun, Y.; Li, D.; Xiao, F.-S.; Liu, J.; Zhang, X. *Chem. Mater.* **2002**, *14*, 1144−1148.

(26) He, N.; Lu, Z.; Yuan, C.; Hong, J.; Yang, C.; Bao, S.; Xu, Q. *Supramol. Sci.* **1998**, *5*, 553−558.

(27) Jun, S.; Kim, J. M.; Ryoo, R.; Ahn, Y.-S.; Han, M.-H. *Microporous Mesoporous Mater.* **2000**, *41*, 119−127.

(28) Mokaya, R. *Angew. Chem., Int. Ed. Engl.* **1999**, *38*, 2930−2934.

(29) Mokaya, R. *Adv. Mater.* **2000**, *12*, 1681−1685.

(30) Mokaya, R. *Chem. Commun.* **2000**, 1891−1892.

(31) Shen, S. C.; Kawi, S. *J. Phys. Chem. B* **1999**, *103*, 8870−8876.

(32) Shen, S. C.; Kawi, S. *Langmuir* **2002**, *18*, 4720−4728.

(33) Zhang, Z.; Han, Y.; Xiao, F.-S.; Qui, S.; Zhu, L.; Wang, R.; Yu, Y.; Zhang, Z.; Zou, B.; Wang, Y.; Sun, H.; Zhao, D.; Wei, Y. *J. Am. Chem. Soc.* **2001**, *123*, 5014−5021.

(34) Zhang, Z.; Han, Y.; Zhu, L.; Wang, R.; Yu, Y.; Qiu, S.; Zhao, D.; Xiao, F.-S. *Angew. Chem., Int. Ed.* **2001**, *40*, 1258−1262.

(35) Pang, J.-B.; Qui, K.-Y.; Wei, Y. *Microporous Mesoporous Mater.* **2000**, *40*, 299−304.

(36) Iler, R. K. *The Chemistry of Silica*; John Wiley and Sons: New York, 1979.

(37) VanCappellen, P.; Qiu, L. *Deep-Sea Res., II* **1997**, *44*, 1129−1149.

(38) Rieker, T. P.; Hubbard, P. F. *Rev. Sci. Instrum.* **1998**, *69*, 3504−3509.

(39) Hietala, S. L.; Smith, D. M.; Hietala, V. M.; Frye, G. C.; Martin, S. J. *Langmuir* **1993**, *9*, 249−251.

(40) Ricco, A. J.; Frye, G. C.; Martin, S. J. *Langmuir* **1989**, *5*, 273−276.

(41) Glaves, C. L.; Frye, G. C.; Smith, D. M.; Brinker, C. J.; Datye, A.; Ricco, A. J.; Martin, S. J. *Langmuir* **1989**, *5*, 459−466.
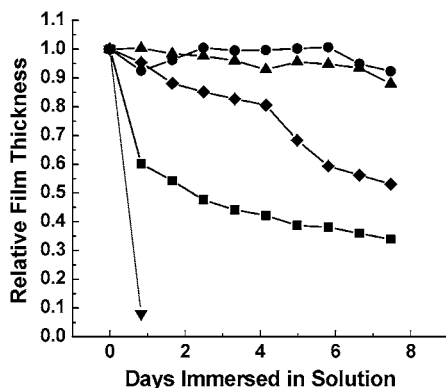
Figure 1. Relative thickness of Al-doped mesoporous silica thin films as a function of immersion time in 10 mM pH 7.4 Tris buffer solution, as determined by ellipsometric measurements. Legend: Al/Si = (▼) 0:1, (■) 1:200, (◆) 1:100, (▲) 1:50, and (●) 1:25.

TEM samples were prepared by scraping the film with a sharp blade and transferring the flakes to a carbon-coated copper grid. Imaging was performed in under-focus conditions.

Results and Discussion

Aqueous Stability of Al-Doped Silica Films. To determine the effect of Al concentration (measured as the molar ratio of Al to Si) on film stability in water, a series of films templated with Brij 56 and with Al/Si ratios from 1:200 to 1:25 were synthesized, keeping the template/Si ratio constant. Aqueous stability was measured by immersion of the samples in 10 mM pH 7.4 Tris buffer; this particular environment was selected because of its relevance in biological and hybrid inorganic/biological materials research. A total of 10 mL of buffer was used per 3.6 cm^2 sample to simulate the semi-infinite dilution conditions that might be encountered in applications such as chemical sensing, yielding a maximum silica solution concentration of ~10 ppm for the films used in these experiments, approximately 1/10th of the maximum silica solubility at pH 7[36] (for this calculation, all silica is assumed to be dissolved, with films of 250 nm thickness and 50% porosity, and a skeletal density of 2.2 g/cm^3). At regular intervals, samples were removed from their buffer solutions and interrogated using spectroscopic ellipsometry to measure film thickness and refractive index, quantities which were then related to film stability. Although the connection between thickness and film degradation is obvious, the refractive index is more difficult to interpret due to (1) adsorption and, at higher humidities, capillary condensation of water in the pore network, and (2) the necessity of knowing the refractive index of the nonporous material in order to approximate the total porosity using an effective medium approximation.[42] On the basis of the results of a previous study on water adsorption inside mesoporous silicate materials,[20] however, it is expected that the former two effects are negligible under our experimental conditions (with typical relative humidities of < 30%). Moreover, as the films within each experiment were characterized under identical environments and compared only on a relative basis, day-to-day variations in water adsorption or condensation can be ignored. Relative comparison also negates the need for optical constants of the nonporous material, as absolute porosities are not being measured.

Figure 1 contains relative thickness data as a function of total immersion time in pH 7.4 buffer for the afore-

(42) Tomkins, H. G.; McGahan, W. A. *Spectroscopic Ellipsometry and Reflectometry*; John Wiley & Sons: New York, 1999.
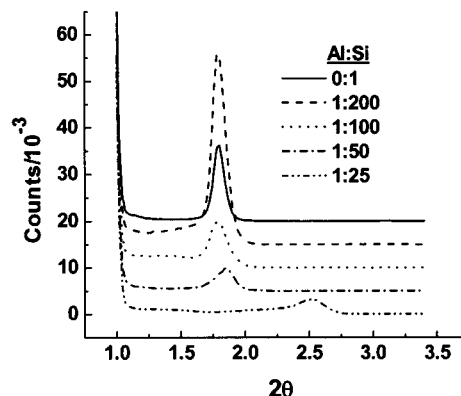
Figure 2. X-ray diffraction patterns of Al-doped mesoporous silica templated with Brij 56 as a function of Al/Si ratio.

mentioned films, demonstrating a strong correlation between Al/Si ratio and film stability. Even addition of 0.5% Al (Al/Si = 1:200) greatly diminishes the rate of film dissolution (for films containing no added Al, the relative thickness dropped to <0.1 within 24 h). Stability appears to maximize at an Al/Si ratio of 1:50; further increases in this ratio have little effect. Over the same time period, there was no significant change in refractive index for any of the films, suggesting that dissolution of the films occurs at the film/solution interface, progressively reducing the film thickness.

As well as increasing film stability in water, addition of Al to a pure silica mesophase can alter the resultant pore structure. For example, as the Al/Si ratio is increased for the data in Figure 1, there are three distinctive shifts in the diffraction pattern as the level of Al doping increases (Figure 2). Without any added Al, a peak is present at ~$2\theta = 1.7°$ which has been attributed to the presence of a 2D hexagonal phase (as confirmed by SAXS measurements). As the molar ratio of Al/Si is raised from 0 to 1:200, there is a significant increase in diffraction peak intensity. Although variations in diffraction peak intensities can occur from variables such as substrate alignment, the data in Figure 2 are reproducible between samples measured under identical conditions, indicating a real effect. This increase in peak intensity may be due to increased electron density contrast between the surfactant (or air, after removal of the surfactant) and oxide phases.

After the Al/Si ratio is increased further (from 1:200 to 1:100), however, there is a dramatic decrease in diffraction peak intensity, followed by a shift in peak position and shape between Al/Si = 1:100 and 1:50. This latter effect can be explained by a hexagonal to cubic phase transformation; SAXS data of films doped with 1:100 Al/Si indicate the presence of a mixed hexagonal/disordered mesostructure, while TEM of films synthesized with Al/Si ratios greater than this shows they are clearly cubic (although with a low degree of ordering), as seen in Figure 3. Although this phase transformation begins at an Al/Si ratio of 1:50, it does not appear to be complete until the Al/Si ratio equals 1:25, where the *d* spacing of the primary diffraction peak is consistent with previous data for cubic phases templated with Brij 56. Although this shift in peak maximum could also be due to film shrinkage, diffraction peak positions do not directly correlate with percent linear film thickness shrinkage during calcination, indicating the absence of this effect.

We have also observed similar structural shifts in films templated with P123; as the Al/Si ratio is increased, cubic phases appear to become more favorable.
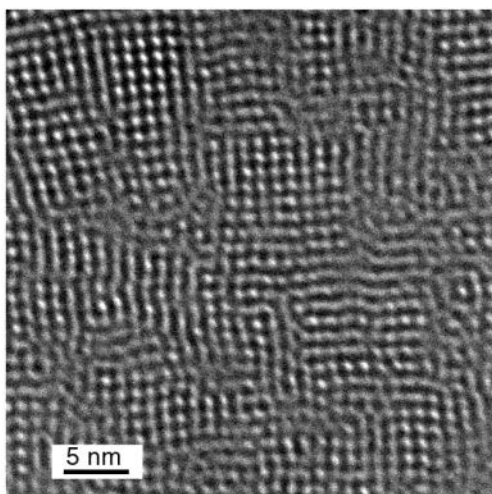
Figure 3. TEM image of a Brij 56 templated silica mesophase, with surfactant/SiO$_2$ mass ratio = 0.94 and Al/Si molar ratio = 1:50, showing a disordered cubic structure.

These structural shifts could be attributed to several phenomena, including pH,[43] changes in ionic interactions between the surfactant and silicate phases during film formation,[44,45] or variations in the degree of silicate condensation.[43] The first effect is likely negligible, however, as the maximum pH differences between sols is at most 0.1, and probably even smaller, leaving the latter two factors as more likely explanations for the observed phase shifts (determination of the precise mechanism is beyond the scope of this communication).

Nitrogen adsorption isotherms, obtained using films deposited on surface acoustic wave (SAW) devices, also indicate changes in pore structure as the Al/Si ratio is increased. Isotherms of Brij 56-templated samples with Al/Si ratios of 0, 1:100, and 1:50 were measured before exposure to water (Figure 4A). Most striking in these data is the apparent decrease in total porosity (a factor of 30–50%) upon introduction of Al. On the basis of refractive index data, however, this decrease is largely due to a reduction in pore accessibility and not pore collapse. Accessible surface area also decreases with Al doping, with surface areas of ~620, 360, and 470 m^2/cm^3 of film volume for Al ratios of 0, 1:100, and 1:50, respectively. Finally, as seen in Figure 4B, the average BJH pore radius decreases from 1.2 nm for pure silica to ~0.9 nm for films with Al, while the BJH pore size distribution widens.

These observed shifts in pore network structure are in complete agreement with many previous literature reports on aluminosilicate powders and films.[15,23,31,32,46] In general, for powdered materials, as Al/Si increases, film order, BET surface area, mesoporosity by N$_2$ adsorption, and average BJH pore size decrease, while the width of the BJH pore size distribution increases. Similar findings have been reported for Al-doped mesoporous silica films templated with octadecyltrimethylammonium chloride,[46] although a lack of good quality N$_2$ adsorption data prohibited adequate comparison of pore volume and surface area between doped and undoped samples.

The precise mechanism whereby aqueous stability is imbued by addition of Al to mesoporous silica is not known.

(43) Gross, A. F.; Ruiz, E. J.; Le, V. H.; Tolbert, S. H. *Microporous Mesoporous Mater.* **2001**, *44–45*, 785–791.
(44) Echchahed, B.; Morin, M.; Blais, S.; Badiei, A.-R.; Berhault, G.; Bonneviot, L. *Microporous Mesoporous Mater.* **2001**, *44–45*, 53–63.
(45) Lin, H. P.; Kao, C. P.; Mou, C. Y. *Microporous Mesoporous Mater.* **2001**, *48*, 135–141.
(46) Ogawa, M.; Kuroda, K.; Mori, J. *Langmuir* **2002**, *18*, 744–749.
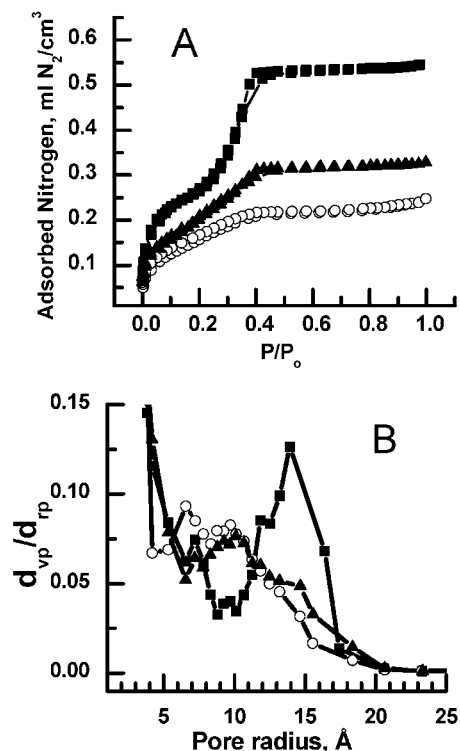
Figure 4. (A) Nitrogen adsorption isotherms for Al-doped Brij 56-templated silica films obtained using a SAW apparatus, plotted as N$_2$ adsorbed per cubic centimeter of film volume to adjust for differing film thicknesses. (B) BJH pore size distributions calculated for this data. Legend: Al/Si = (■) 0:1, (▲) 1:100, and (○) 1:50.

One explanation for the increased aqueous stability of aluminosilicate materials over that of pure silica is decreased net surface charge;[15,47] as the dissolution rate of silica is believed to be proportional to the density of negative charge,[47] addition of Al species (which are positively charged below a pH of ca. 8) decreases this rate due to charge cancellation. Assuming a homogeneous distribution of Al inside the silica phase, however, the net surface charge should only be decreased by ~4% for even the highest Al/Si ratio investigated (1:25), too low of a change to significantly affect the dissolution rate given a linear dependence of surface charge on dissolution kinetics. Alternatively, it is possible that Al species are concentrated at the surfactant/silicate interface during mesophase formation. Measurement of surface charge (and thus distribution of Al species) in these materials is left for future investigation, however.

Other potential explanations for the observed stability of Al-doped silica mesostructures include reduced solubility of aluminosilicate species relative to Si(OH)$_4$, increased siloxane condensation due to decrease in sol pH from addition of AlCl$_3$, and modifications to the reactivity of siloxane bonds compared to undoped silicate materials.[15,32] The last phenomenon is intriguing in light of recent Raman studies on surfactant-templated films demonstrating the presence of small silicate rings inside surfactant-templated films.[48] These strained structures are significantly more reactive toward hydrolysis than silica,[49] an effect that may account for the poor hydrolytic stability of surfactant-templated silica films compared to nonporous materials (as confirmed by a simple experiment, films synthesized

(47) Brady, P. V.; Walther, J. V. *Chem. Geol.* **1990**, *82*, 253–264.
(48) Fan, H. Y.; Brinker, C. J. *Nature*, submitted for review.
(49) Bunker, B. C. *J. Non-Cryst. Solids* **1994**, *179*, 300–308.
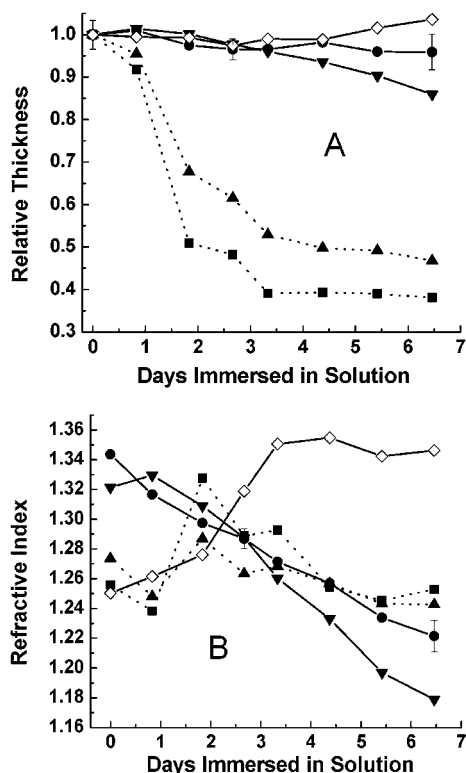
Figure 5. (A) Comparison of the relative thickness of Al-doped films templated with Brij 56, P123, or CTAB, at two different surfactant/SiO_2 mass ratios, as a function of immersion time in 10 mM pH 7.4 Tris buffer solution. (B) Refractive index for these films. Legend for both panels: SiO_2/P123 mass ratio = (■) 1.06 and, (●) 2.12. SiO_2/Brij 56 mass ratio = (▲) 1.06 and (▼) 2.12. SiO_2/CTAB mass ratio = (◇) 2.12. Typical error bars (at the 95% confidence level) have been added to data for SiO_2/P123 mass ratio = 2.12.

without any surfactant template but under otherwise identical conditions did not exhibit the rapid degradation in water seen for surfactant-templated films). Although it is pure speculation at this point, addition of Al species may suppress the formation of these unstable structures. Finally, the physical properties of the pore network (surface area, pore accessibility, pore size, mesophase curvature, etc.) may be contributing factors to film solubility, especially given the observation that nontemplated SiO_2 sol–gel films are significantly more stable than surfactant-templated ones. For this reason, we wished to determine if the structure of the pore network inside surfactant templated films is an important variable for relative film solubility.

To this end, an experiment was designed to probe the effect of template type and concentration (and thus mesopore structure) on film dissolution kinetics. A series of films were synthesized with three different types of surfactants (ionic, nonionic, and block copolymer, represented by CTAB, Brij 56, and P123, respectively) at two different surfactant/SiO_2 mass ratios. An intermediate Al/Si ratio (1:100) was selected in order to confer only moderate aqueous stability to the films, increasing the sensitivity of dissolution kinetics to structural factors. Figure 5A contains thickness data as a function of immersion time in pH 7.4 buffer for these films. Interestingly, the data can be grouped into two narrow behavioral regimes based on the surfactant/Si weight ratio, one with high and one with intermediate thickness stability. Given the differences in pore diameter typically found in materials templated with these three surfactants (<2 nm

for CTAB, 2–3 nm for Brij 56, and 7–8 nm for P123),[50] and their similarity in solubility behavior, pore size can be ruled out as contributing to the differential thickness stability seen in Figure 5A. Furthermore, as the surface area at constant surfactant/SiO_2 weight ratio increases with decreasing pore size, surface area can also be dismissed as a major influence of dissolution rate in these materials.

Film internal stability, as measured by refractive index, is given in Figure 5B. Again, the data (with the exception of that for CTAB) fall into two groups, although the observed behavior is the inverse of that seen for thickness stability. Mesoporous aluminosilicate films formed with surfactant/Si mass ratios = 0.94 show poor internal stability while those with the surfactant/Si ratio = 0.47 have little variation in refractive index over the same period. The data for CTAB are an anomaly, in that the refractive index increases significantly during the experiment. Although the reason for this increase is unknown, it is likely an effect of water adsorption. The smaller pore size and higher surface area of CTAB-templated materials (compared to materials templated with Brij 56 or P123) increase the susceptibility toward adsorption or capillary condensation of water in the pore network.

Although surface area and pore size do not appear to be the primary properties that determine the film dissolution behavior observed in Figure 5, mesophase identity is. Mesophase structure was determined for Brij 56-, P123-, and CTAB-templated films identical to those used to generate the data in Figure 5 using GISAXS and X-ray reflectivity. Brij 56-, P123-, and CTAB-templated films with high thickness stability were identified as having cubic (Brij 56, P123 templates) or disordered "worm-hole" (CTAB) phases, while Brij 56 and P123 templated films with low thickness stability were found to be largely hexagonal (with a significant fraction of a disordered phase also present). Given these structures, a few explanations for the observed differences in film dissolution behavior can be hypothesized. First, as the pores in the hexagonal films are largely parallel to the surface (as determined from GISAXS data), pore accessibility to solution may be a significant factor, although on the basis of this argument one would expect 3D phases to be less stable. Also, 3D (cubic, disordered) and 2D (hexagonal) phases possess different net curvatures (zero for cubic phases, positive for hexagonal phases); the resulting differences in interfacial energies may control film solubility, at least in part.[36]

Grafting of $Al(H_2O)_6^{3+}$ onto Preformed Silica Mesophases. A second method of incorporating aluminum oxide species into mesostructured silica films is by postsynthesis grafting using aqueous solutions of $AlCl_3 \cdot 6H_2O$. Figure 6 presents the results of a study where film stability, as monitored by ellipsometric measurements, is measured as a function of grafting time of mesoporous silica films in 0.5 M $AlCl_3 \cdot 6H_2O$. From these data, it is readily apparent that, even at grafting times as short as 1 h, film thickness is not affected by immersion in buffer solution. Internal stability, however, is a strong function of grafting time. For all samples, there is a significant increase in refractive index after 1 day in buffer solution; this can be attributed to adsorption of water into the pore network (addition of acidic Al sites inside the mesostructure may increase this effect). After this initial process, the refractive index decreases for all films, even for samples grafted for 11 h. However, the magnitude of this change, measured from either the initial or maximum refractive

(50) Fan, H. Y. *Chemical and Nuclear Engineering*; University of New Mexico: Albuquerque, 2000; p 178.
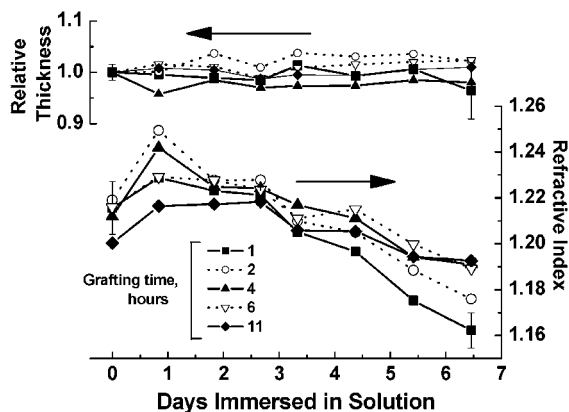
Figure 6. Relative thickness (top) and refractive index (bottom) for Al-grafted mesoporous silica films, reacted for different lengths of time, versus days immersed in 10 mM pH 7.4 Tris buffer. Typical error bars (at the 95% confidence level) have been added to data from a grafting time of 1 h.

index, is highly dependent on $AlCl_3 \cdot 6H_2O$ reaction time; for samples grafted for 6 h, Δn is less than 0.03 from the initial refractive index or 0.04 from the maximum.

The Al/Si ratio for films grafted for 4 h was measured by first dissolving a set of treated films in pH ~ 10 water, followed by analyses of $Si(OH)_4$ with the β silicomolybdate method[36] and of dissolved Al by a fluorometric assay of the 8-hyroxyquinoline complex of aluminum.[51] The ratio of Al/Si was determined to be 0.026 ± 0.009 (68% probability), a similar number to the ratio of Al/Si in Al-doped films where maximum aqueous stability is obtained.

The internal stability of grafted films may be slightly less than that of Al-doped films over the period of ~1 week, and film synthesis involves extra steps, but there may be advantages to this route in that film structure is perturbed less by grafting relative to direct synthesis. For example, after 6 h of grafting followed by the second heat treatment at 450 °C (necessary for imbuing stability in templated films using this grafting route),the d spacing of the cubic mesophase shrank by only ~3% (as determined by X-ray diffraction), while fwhm peak width increased by less than 30%. These observed shifts are at least in part due to increased thermal treatment time in addition to Al grafting. Prolonged thermal treatment may also increase siloxane condensation, adding to aqueous stability. Pure surfactant-templated SiO_2 films calcined a second

time without a grafting step still were found to be as unstable in water as those only calcined a single time, however. At present, the effect of Al grafting on pore size and accessibility in thin films is not known, and this remains a topic of further research.

Conclusions

To prevent dissolution of surfactant-templated silica films in water, aluminum species have been introduced into silica mesophases either by addition of alumina precursors to the precursor sol or by grafting with $AlCl_3 \cdot 6H_2O$ followed by thermal treatment. In the direct synthesis route, addition of even 1:50 Al/Si stabilizes films such that only 10% of the film thickness is lost after 1 week in pH 7.4 Tris buffer solution. Doping with Al can potentially also perturb the mseostructure identity, as shown for the case of Brij 56-templated films, inducing changes in mesophase type while decreasing accessible mesopore volume and surface area. The solubility behavior of silicate films doped with 1% Al appears to be sensitive to mesophase identity, with 3D phases (cubic, disordered) dissolving from within the film, while hexagonal (2D) films dissolve at the film/solution interface. Grafting with $AlCl_3 \cdot 6H_2O$ also dramatically increases film stability, at the cost of added processing steps. The internal stability for grafted films is not as high as that seen for aluminosilicate films prepared by direct synthesis.

A fundamental issue that is not discussed here, but is worthy of further study, is the effect of water exposure on mesopore structure in aluminosilicate films. Another important area for future research concerns the speciation and location of alumina species in both doped and grafted films, both questions where X-ray photoelectron spectroscopy (XPS) may be of use. Finally, other metal oxides may endow similar aqueous stability in mesoporous silica films; identification of these metals and characterization of the resultant doped or grafted silica films may prove fruitful.

(51) Peterson, J. *J. Chem. Educ.* **1996**, *73*, 262–264.